

# Forced vibration of the elastic system consisting of the hollow cylinder and surrounding elastic medium under perfect and imperfect contact

Surkay D. Akbarov<sup>\*1,2</sup> and Mahir A. Mehdiyev<sup>2,3a</sup>

<sup>1</sup>Department of Mechanical Engineering, Yildiz Technical University, Istanbul, Turkey

<sup>2</sup>Institute of Mathematics and Mechanics of NAS Azerbaijan, Baku, Azerbaijan

<sup>3</sup>Azerbaijan State Economics University, Department of Mathematics, Baku, Azerbaijan

(Received October 18, 2016, Revised February 11, 2017, Accepted February 13, 2017)

**Abstract.** The bi-material elastic system consisting of the circular hollow cylinder and the infinite elastic medium surrounding this cylinder is considered and it is assumed that on the inner free face of the cylinder a point-located axisymmetric time harmonic force, with respect to the cylinder's axis and which is uniformly distributed in the circumferential direction, acts. The shear-spring type imperfect contact conditions on the interface between the constituents are satisfied. The mathematical formulation of the problem is made within the scope of the exact equations of linear elastodynamics. The focus is on the frequency-response of the interface normal and shear stresses and the influence of the problem parameters, such as the ratio of modulus of elasticity, the ratio of the cylinder thickness to the cylinder radius, and the shear-spring type parameter which characterizes the degree of the contact imperfectness, on these responses. Corresponding numerical results are presented and discussed. In particular, it is established that the character of the influence of the contact imperfectness on the frequency response of the interface stresses depends on the values of the vibration frequency of the external forces.

**Keywords:** forced vibration; frequency response; hollow cylinder; surrounding elastic medium; shear-spring type imperfectness; underground structure

## 1. Introduction

It is known that in many cases, pipelines, tunnels, subway lining, mine works and other similar types of underground structures can be modelled as infinite hollow cylinders surrounded with an elastic or viscoelastic infinite medium. Consequently, the theoretical study of the problems related to the dynamics of the soil-structure interaction can be carried out with the use of the mechanical model consisting of a hollow cylinder and surrounding elastic or viscoelastic medium. In connection with this, in the present work we investigate the forced vibration of this system under action of the point-located axisymmetric normal forces, with respect to the cylinder axis which are uniformly distributed in the circumferential direction, acting on the inner surface of the cylinder. However, up to now in related investigations, the focus has been on the study of the resonance waves in such systems. For instance, in the paper by Abdulkadirov (1981) and others listed therein, the low-frequency resonance axisymmetric longitudinal waves in a cylindrical layer surrounded by an elastic medium are investigated. Note that under "resonance waves" it is understood that the velocity of the waves is determined from the relation  $dc/dk=0$ , where  $c$  is the wave propagation

velocity and  $k$  is the wavenumber. It is evident that the resonance velocity corresponds to the point of the dispersion curves at which the tangential line to this curve is parallel to the wavenumber axis. In the paper by Abdulkadirov (1981) it is established that if the modulus of elasticity of the cylinder material is greater than that of the surrounding elastic material then the aforementioned resonance waves appear. Moreover, in that paper it is established that the character of the contact conditions (in the sense of the perfect and imperfect) between the cylinder and surrounding medium also has a great influence on the dispersion curves. In connection with this, it is found that under imperfect (full slipping) contact between the constituents, the long waves limit value of the wave propagation velocity exists in the lowest first mode. However, this limit value does not exist under perfect contact between the constituents. In this sense, we note that the influence of the imperfect contact conditions on the axisymmetric and flexural wave dispersion in compound cylinders was also studied in the papers by Akbarov and Ipek (2012, 2015), Ipek (2015) and detailed in the monograph by Akbarov (2015), in which it was established that the imperfectness of the contact conditions between the constituents can influence the dispersion curves not only quantitatively, but also qualitatively. Moreover, we note that the velocity of the resonance waves determined in the paper by Abdulkadirov (1981) and others listed therein coincides with the critical velocity of the axisymmetric moving load acting on the inner surface of the hollow cylinder and under this velocity the resonance type phenomenon takes place. A review of the investigations regarding the dynamics of the

\*Corresponding author, Professor

E-mail: [akbarov@yildiz.edu.tr](mailto:akbarov@yildiz.edu.tr)

<sup>a</sup>Ph.D.

E-mail: [mahirmehdiyev@mail.ru](mailto:mahirmehdiyev@mail.ru)

moving load acting on the layered system has been made in the monograph by Akbarov (2015) and related papers listed therein. According to these investigations, it was established that under action of the moving load on the layered half-space, the critical velocity appears only in the cases where the modulus of elasticity of the covering layer material is greater than that of the half-space material. Consequently, the condition on the existence of the critical velocity for the plane-layered systems coincides with the corresponding one examined in the paper by Abdulkadirov (1981).

Note that vibration problems for the hollow cylinders and spheres without any connection with the surrounding medium are considered in the papers by Asgari *et al.* (2011), Hasheminejad and Mirzaei (2011), Baba and Keles (2016), Bayon *et al.* (2012), Ebenezer *et al.* (2015), Kharouf and Heyliger (1994) and other ones listed therein.

The other type of problems related to the layered systems are the problems related to their forced vibration. Up to now, such types of problems are investigated mainly for the plane-layered systems. The source of these investigations is Lamb's (1904) paper in which the time-harmonic Lamb's problem was investigated and it was established that the frequency response of the stresses have non-monotonic character. In other words, in the paper by Lamb (1904) it was established that the behavior of the half-space under time harmonic forced vibration is similar to the behavior of the discrete mechanical system consisting of the spring, mass and parallel connected dashpot. Later, this conclusion was also established with the investigations by Gladwell (1968), Johnson (1985), Wang and Achenbach (1996) and others. The corresponding investigations regarding the layered half space, or more-precisely, regarding the system consisting of the half-space and covering layer started in the first decades of the XXI century and have continued up to now by the first author of the present paper and his students. Consider a brief review of some of these investigations which are also detailed in the monograph by Akbarov (2015). We begin this review with the paper by Akbarov (2006a) in which the axisymmetric forced vibration problem for the system consisting of the finitely pre-strained half-space and finitely pre-strained covering layer is studied and it is assumed that this forced vibration is caused by the point-located time-harmonic normal force acting on the free-face plane of the covering layer. The three-dimensional linearized equations of the theory of elastic waves in initially stressed bodies are employed for mathematical formulation of the problem. It is supposed that the materials of the constituents are incompressible and their elasticity relations are described through the Treloar potential. In the case where the initial stresses (or strains) are equated to zero, the problem formulation and obtained concrete numerical results relate to the corresponding ones obtained within the scope of the classical linear theory of elastodynamics. Numerical results on the frequency response of the interface stresses are presented and discussed. It is established that the mechanical behavior of the axisymmetric forced vibration of the system consisting of the covering layer and half-space is also similar to that for the system consisting of a spring, mass and parallel connected dashpot.

In the other paper by Akbarov (2006b), within the scope of the assumptions and field equations used in the paper by Akbarov (2006a) the forced vibration of the pre-strained bi-layered slab resting on the rigid foundation is examined. It is found that under axisymmetric forced vibration of the bi-layered slab resting on the rigid foundation, ordinary resonance frequencies appear and consequently the vibration of the system under consideration is dissimilar from the vibration of the system consisting of a spring, mass and parallel connected dashpot.

In the paper by Akbarov and Guler (2007) the forced vibration of the system consisting of a pre-stressed half-plane and pre-stressed covering layer under action of the linearly-located inclined time-harmonic forces is studied. It is assumed that the initial strains are small and the initial static stress-strain state is determined within the scope of the classical linear theory of elasticity. Concrete numerical results are presented for aluminum and steel and according to these results it is also established that the behavior of the system under consideration is similar to the corresponding behavior of the system comprising a spring, mass and parallel connected dashpot.

In all the foregoing investigations, it is assumed that the materials of the covering layer and half-space are isotropic. In the papers by Akbarov and Ilhan (2010, 2013), and Ilhan and Koc (2015) the aforementioned investigations are developed for the cases where the materials of the constituents are orthotropic (Akbarov and Ilhan 2010) and piezoelectric (Akbarov and Ilhan 2013).

With this we restrict our review of the investigations related to the forced vibration of plane-layered bi-material elastic systems. At the same time, we recall that a more detailed review and consideration of the results reviewed above can be found in the monograph by Akbarov (2015).

Thus, it follows from the foregoing review that up to now there has not been any investigations related to the forced vibration of elastic systems consisting of the cylindrical covering layer and infinite elastic medium surrounding this layer. Taking into consideration this statement and the significance of the results of related theoretical investigations for understanding the dynamics of underground structures, in the present paper we attempt to investigate an axisymmetric forced vibration of the system comprising the circular hollow cylinder and surrounding infinite elastic medium under action of the point-located axisymmetric time-harmonic normal forces, with respect to the cylinder axis, uniformly distributed in the circumferential direction on the inner surface of the cylinder. Consequently, the problem studied in the present paper can also be considered as a development of the reviewed-above investigations for cylindrically-layered bi-material elastic systems.

## 2. Mathematical formulation of the problem

Consider a system consisting of the hollow circular cylinder with thickness  $h$  and surrounding infinite elastic medium and associated with the central axis of this cylinder are the cylindrical and Cartesian systems of coordinates

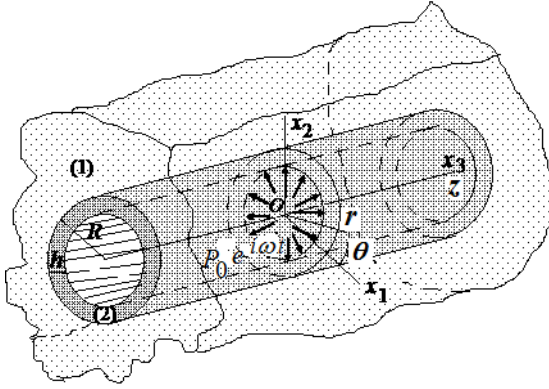


Fig. 1 The sketch of the elastic system under consideration

$O r \theta z$  and  $O x_1 x_2 x_3$  (Fig. 1). Assume that the external radius of the cross section of the cylinder is  $R$  and that at the point  $z=0$  on the inner surface of the cylinder, in the circumferential direction, uniformly distributed axisymmetric time-harmonic normal forces act. Within these frameworks we investigate the axisymmetric frequency response of this system to these forces by employing the exact equations of the linear theory of elastodynamics. Below, the values related to the cylinder and to the surrounding elastic medium will be denoted by upper indices (2) and (1), respectively.

Assume that the materials of the constituents are homogeneous and isotropic. We write the field equations and contact conditions.

Equations of motion

$$\begin{aligned} \frac{\partial \sigma_{rr}^{(k)}}{\partial r} + \frac{\partial \sigma_{rz}^{(k)}}{\partial z} + \frac{1}{r}(\sigma_{rr}^{(k)} - \sigma_{\theta\theta}^{(k)}) &= \rho^{(k)} \frac{\partial^2 u_r^{(k)}}{\partial t^2}, \\ \frac{\partial \sigma_{rz}^{(k)}}{\partial r} + \frac{\partial \sigma_{zz}^{(k)}}{\partial z} + \frac{1}{r} \sigma_{rz}^{(k)} &= \rho^{(k)} \frac{\partial^2 u_z^{(k)}}{\partial t^2}. \end{aligned} \quad (1)$$

Elasticity relations

$$\begin{aligned} \sigma_{mn}^{(k)} &= \lambda^{(k)}(\varepsilon_{rr}^{(k)} + \varepsilon_{\theta\theta}^{(k)} + \varepsilon_{zz}^{(k)}) + 2\mu^{(k)}\varepsilon_{mn}^{(k)}, \\ mn &= rr; \theta\theta; zz, \quad \sigma_{rz}^{(k)} = 2\mu^{(k)}\varepsilon_{rz}^{(k)} \end{aligned} \quad (2)$$

Strains-displacement relations

$$\begin{aligned} \varepsilon_{rr}^{(k)} &= \frac{\partial u_r^{(k)}}{\partial r}, \quad \varepsilon_{\theta\theta}^{(k)} = \frac{u_r^{(k)}}{r}, \quad \varepsilon_{zz}^{(k)} = \frac{\partial u_z^{(k)}}{\partial z}, \\ \varepsilon_{rz}^{(k)} &= \frac{1}{2} \left( \frac{\partial u_z^{(k)}}{\partial r} + \frac{\partial u_r^{(k)}}{\partial z} \right) \end{aligned} \quad (3)$$

Thus, the Eqs. (1), (2) and (3) are the complete system of the field equations of the linear theory of elastodynamics in the case under consideration and in these equations conventional notation is used.

Now we consider the formulation of the boundary and contact conditions. According to the foregoing description of the problem, the boundary conditions on the inner face surface of the cylinder can be formulated as follows.

$$\sigma_{rr}^{(2)} \Big|_{r=R-h} = -P_0 \delta(z) e^{i\omega t}, \quad \sigma_{rz}^{(2)} \Big|_{r=R-h} = 0 \quad (4)$$

We assume that the contact conditions with respect to the forces and radial displacement are continuous and can be written as follows

$$\begin{aligned} \sigma_{rr}^{(1)} \Big|_{r=R} &= \sigma_{rr}^{(2)} \Big|_{r=R}, \quad \sigma_{rz}^{(1)} \Big|_{r=R} = \sigma_{rz}^{(2)} \Big|_{r=R}, \\ u_r^{(1)} \Big|_{r=R} &= u_r^{(2)} \Big|_{r=R} \end{aligned} \quad (5)$$

At the same time, we assume that the shear-spring type imperfection occurs in the contact conditions related to the axial displacements and, according to Berger *et al.* (2000), Akbarov and Ipek (2012, 2015) and others listed therein, these conditions are formulated by the following equation

$$u_z^{(2)} \Big|_{r=R} - u_z^{(1)} \Big|_{r=R} = \frac{FR}{\mu^{(1)}} \sigma_{rz}^{(1)} \Big|_{r=R} \quad (6)$$

The dimensionless parameter  $F$  in (6) characterizes the degree of the imperfection and the range of change of this parameter is  $-\infty \leq F \leq \infty$ . Note that the case where  $F=0$  corresponds to complete contact, but the case where  $F=\pm\infty$  corresponds to full slipping contact conditions.

Moreover, we assume that

$$\begin{aligned} \left| \sigma_{rr}^{(1)} \right|; \left| \sigma_{\theta\theta}^{(1)} \right|; \left| \sigma_{zz}^{(1)} \right|; \left| \sigma_{rz}^{(1)} \right|; \left| u_r^{(1)} \right|; \left| u_z^{(1)} \right| &< M = \text{const.} \\ \text{as } \sqrt{r^2 + z^2} &\rightarrow \infty \end{aligned} \quad (7)$$

This completes formulation of the problem and consideration of the governing field equations.

### 3. Method of solution

For solution to the problem formulated above we use the well-known, classical Lamé (or Helmholtz) decomposition (see, for instance, Eringen and Suhubi 1975)

$$\begin{aligned} u_r^{(k)} &= \frac{\partial \Phi^{(k)}}{\partial r} + \frac{\partial^2 \Psi^{(k)}}{\partial r \partial z}, \\ u_z^{(k)} &= \frac{\partial \Phi^{(k)}}{\partial z} + \frac{\partial^2 \Psi^{(k)}}{\partial z^2} - \frac{1}{(c_2^{(k)})^2} \frac{\partial^2 \Psi^{(k)}}{\partial t^2} \end{aligned} \quad (8)$$

where  $\Phi^{(k)}$  and  $\Psi^{(k)}$  satisfy the following equations

$$\begin{aligned} \nabla^2 \Phi^{(k)} - \frac{1}{(c_1^{(k)})^2} \frac{\partial^2 \Phi^{(k)}}{\partial t^2} &= 0, \\ \nabla^2 \Psi^{(k)} - \frac{1}{(c_2^{(k)})^2} \frac{\partial^2 \Psi^{(k)}}{\partial t^2} &= 0, \quad \nabla^2 = \frac{\partial^2}{\partial r^2} + \frac{1}{r} \frac{\partial}{\partial r} + \frac{\partial^2}{\partial z^2}, \end{aligned} \quad (9)$$

$$c_2^{(k)} = \sqrt{\mu^{(k)}/\rho^{(k)}}, \quad c_1^{(k)} = \sqrt{(\lambda^{(k)} + \mu^{(k)})/\rho^{(k)}}$$

As we consider the time-harmonic forced vibration of the above described system under action of the force  $P_0 \delta(z) e^{i\omega t}$ , we can represent all the sought values as  $g(r, z, t) = \bar{g}(r, z) e^{i\omega t}$ . According to this representation, we obtain the corresponding equations, boundary and contact conditions for the amplitudes of the displacements and stresses from the foregoing equations by replacing the

operator  $\partial^2 f / \partial r^2$  with  $-\omega^2 \bar{f}$ . Below we will omit the over-bar on the amplitudes.

Thus, using the dimensionless coordinates  $r'=r/h$  and  $z'=z/h$  (the upper prime will be omitted below) and introducing the notation

$$\Omega = \frac{\omega h}{c_2^{(2)}} \quad (10)$$

we obtain the following equations for the amplitudes of the potentials  $\Phi^{(k)}$  and  $\Psi^{(k)}$

$$\left( \frac{\partial^2}{\partial r^2} + \frac{1}{r} \frac{\partial}{\partial r} + \frac{\partial^2}{\partial z^2} + \frac{\Omega^2 c_2^{(2)}}{c_1^{(k)}} \right) \Phi^{(k)} = 0, \quad (11)$$

$$\left( \frac{\partial^2}{\partial r^2} + \frac{1}{r} \frac{\partial}{\partial r} + \frac{\partial^2}{\partial z^2} + \frac{\Omega^2 c_2^{(2)}}{c_2^{(k)}} \right) \Psi^{(k)} = 0$$

For solution to the equations in (11) and other foregoing equations rewritten for the amplitudes we employ the exponential Fourier transformation to these equations with respect to the coordinate  $z$ .

$$f_F = \int_{-\infty}^{+\infty} f(z) e^{izs} dz \quad (12)$$

Thus, after employing this transformation, we obtain the following equations for  $\Phi_F^{(k)}$  and  $\Psi_F^{(k)}$ .

$$\left( \frac{\partial^2}{\partial r^2} + \frac{1}{r} \frac{\partial}{\partial r} + \frac{\Omega^2 c_2^{(2)}}{c_1^{(k)}} - s^2 \right) \Phi_F^{(k)} = 0, \quad (13)$$

$$\left( \frac{\partial^2}{\partial r^2} + \frac{1}{r} \frac{\partial}{\partial r} + \frac{\Omega^2 c_2^{(2)}}{c_2^{(k)}} - s^2 \right) \Psi_F^{(k)} = 0$$

Moreover, after employing this transformation, the second condition in (4) and all the conditions in (5) and (6) remain as are for the Fourier transformation of the corresponding quantities. However, the transformation of the first condition in (4) becomes

$$\sigma_{rr}^{(2)} \Big|_{r=R-h} = -P_0. \quad (14)$$

Solutions to the equations in (13) are

$$\begin{aligned} \Phi_F^{(2)} &= A_1 H_0^{(1)}(r_1) + A_2 H_0^{(2)}(r_1), \\ \Psi_F^{(2)} &= B_1 H_0^{(1)}(r_2) + B_2 H_0^{(2)}(r_2), \\ \Phi_F^{(2)} &= C_2 H_0^{(2)}(r_{11}), \quad \Psi_F^{(2)} = D_2 H_0^{(2)}(r_{21}) \end{aligned} \quad (15)$$

where  $H_0^{(1)}(x)$  and  $H_0^{(2)}(x)$  are the Hankel functions of the first and second kinds, respectively and

$$\begin{aligned} r_1 &= r \sqrt{\Omega^2 \delta_1^2 - s^2}, \quad \delta_1 = \frac{c_2^{(2)}}{c_1^{(2)}}, \quad r_2 = r \sqrt{\Omega^2 - s^2}, \\ r_{11} &= r \sqrt{\Omega_1^2 \delta_2^2 - s^2}, \quad \Omega_1 = \Omega \frac{c_2^{(2)}}{c_2^{(1)}}, \quad r_{21} = r \sqrt{\Omega_1^2 - s^2} \end{aligned} \quad (16)$$

Substituting the solutions (15) and (16) into the Fourier transformations of the presentations for the displacements in (8), the strain-displacement relations in (3) and the elasticity relations in (2), we obtain the following expressions for the transformations of the stresses and displacements which enter into the boundary and contact conditions.

$$\begin{aligned} u_{rF}^{(2)} &= -A_1 \frac{dr_1}{dr} H_1^{(1)}(r_1) - A_2 \frac{dr_1}{dr} H_1^{(2)}(r_1) + \\ &B_1 \frac{dr_2}{dr} is H_1^{(1)}(r_2) + B_2 \frac{dr_2}{dr} is H_1^{(2)}(r_2), \\ u_{zF}^{(2)} &= -A_1 is H_0^{(1)}(r_1) - A_2 is H_0^{(2)}(r_1) + \\ &B_1 (\Omega^2 - s^2) H_0^{(1)}(r_2) + B_2 (\Omega^2 - s^2) H_0^{(2)}(r_2), \\ \sigma_{rrF}^{(2)} &= \mu^{(2)} \left[ A_1 \left( -1 + \frac{\lambda^{(2)}}{2\mu^{(2)}} \right) \left( \frac{dr_1}{dr} \right)^2 (H_0^{(1)}(r_1) \right. \right. \\ &\left. \left. - H_2^{(1)}(r_1)) - \frac{\lambda^{(2)}}{\mu^{(2)}} \frac{dr_1}{dr} H_1^{(1)}(r_1) - \frac{\lambda^{(2)}}{\mu^{(2)}} s^2 H_0^{(1)}(r_1) \right) \right. \\ &\left. + A_2 \left( -1 + \frac{\lambda^{(2)}}{2\mu^{(2)}} \right) \left( \frac{dr_1}{dr} \right)^2 (H_0^{(2)}(r_1) - H_2^{(2)}(r_1)) \right. \\ &\left. - \frac{\lambda^{(2)}}{\mu^{(2)}} \frac{dr_1}{dr} H_1^{(2)}(r_1) - \frac{\lambda^{(2)}}{\mu^{(2)}} s^2 H_0^{(2)}(r_1) \right) + \\ &B_1 \left( -1 + \frac{\lambda^{(2)}}{2\mu^{(2)}} \right) \left( \frac{dr_2}{dr} \right)^2 is (H_0^{(1)}(r_2) - H_2^{(1)}(r_2)) \\ &\left. + \frac{\lambda^{(2)}}{\mu^{(2)}} \frac{1}{r} \frac{dr_2}{dr} is H_1^{(1)}(r_2) - \right. \\ &\left. \frac{\lambda^{(2)}}{\mu^{(2)}} is (\Omega^2 - s^2) H_0^{(1)}(r_2) \right) + \\ &B_2 \left( -1 + \frac{\lambda^{(2)}}{2\mu^{(2)}} \right) \left( \frac{dr_2}{dr} \right)^2 is (H_0^{(2)}(r_2) - H_2^{(2)}(r_2)) \\ &\left. + \frac{\lambda^{(2)}}{\mu^{(2)}} \frac{1}{r} \frac{dr_2}{dr} is H_1^{(2)}(r_2) - \frac{\lambda^{(2)}}{\mu^{(2)}} is (\Omega^2 - s^2) H_0^{(2)}(r_2) \right) \Big], \\ \sigma_{rzF}^{(2)} &= \mu^{(2)} \left[ A_1 \frac{dr_1}{dr} 2is H_1^{(1)}(r_1) + \right. \\ &A_2 \frac{dr_1}{dr} 2is H_1^{(2)}(r_1) + B_1 \frac{dr_2}{dr} (2s^2 - \Omega^2) H_1^{(1)}(r_2) \\ &\left. + B_2 \frac{dr_2}{dr} (2s^2 - \Omega^2) H_1^{(2)}(r_2) \right], \\ u_{rF}^{(1)} &= -C_2 \frac{dr_{11}}{dr} H_1^{(2)}(r_{11}) + D_2 \frac{dr_{21}}{dr} is H_1^{(2)}(r_{21}), \\ u_{zF}^{(1)} &= -C_2 is H_0^{(2)}(r_{11}) + D_2 (\Omega_1^2 - s^2) H_0^{(2)}(r_{21}), \\ \sigma_{rrF}^{(1)} &= \mu^{(1)} \left[ C_2 \left( -1 + \frac{\lambda^{(1)}}{2\mu^{(1)}} \right) \left( \frac{dr_{11}}{dr} \right)^2 \times \right. \\ &\left. (H_0^{(2)}(r_{11}) - H_2^{(2)}(r_{11})) - \right. \end{aligned} \quad (17)$$

$$\begin{aligned}
 & \frac{\lambda^{(1)}}{\mu^{(1)}} \frac{dr_{11}}{dr} H_1^{(2)}(r_{11}) - \frac{\lambda^{(1)}}{\mu^{(1)}} s^2 H_0^{(2)}(r_{11}) + \\
 & D_2 \left( -1 + \frac{\lambda^{(1)}}{2\mu^{(1)}} \left( \frac{dr_{21}}{dr} \right)^2 \right) is(H_0^{(2)}(r_{21}) \\
 & - H_2^{(2)}(r_{21})) + \frac{\lambda^{(1)}}{\mu^{(1)}} \frac{1}{r} \frac{dr_{21}}{dr} isH_1^{(2)}(r_{21}) - \\
 & \left. \frac{\lambda^{(1)}}{\mu^{(1)}} is(\Omega^2 - s^2) H_0^{(2)}(r_{21}) \right], \\
 & \sigma_{rzF}^{(1)} = \mu^{(1)} \left[ C_2 \frac{dr_{11}}{dr} 2isH_1^{(2)}(r_{11}) + \right. \\
 & \left. D_2 \frac{dr_{21}}{dr} (2s^2 - \Omega_1^2) H_1^{(2)}(r_{21}) \right]
 \end{aligned}$$

Thus, substituting the expressions in (17) into the Fourier transformation of the boundary and contact conditions (4)-(6), we obtain the following equations for the unknowns  $A_1, A_2, B_1, B_2, C_2$  and  $D_2$ .

$$\begin{aligned}
 & A_1 \alpha_{1j} + A_2 \alpha_{2j} + B_1 \alpha_{3j} + B_2 \alpha_{4j} +, \\
 & C_2 \alpha_{5j} + D_2 \alpha_{6j} = -P_0 \delta_j^1, \quad j = 1, 2, \dots, 6.
 \end{aligned} \quad (18)$$

Note that the explicit expression of the coefficients  $\alpha_{mj}$  ( $m, j=1, 2, \dots, 6$ ) can be easily determined from the expressions in (6) and (17). It is evident that the solution to the equation (18) can be presented as follows.

$$\begin{aligned}
 & A_1 = \frac{\det(\beta_{mj}^{(1)})}{\det(\alpha_{mj})}, \quad A_2 = \frac{\det(\beta_{mj}^{(2)})}{\det(\alpha_{mj})}, \\
 & B_1 = \frac{\det(\beta_{mj}^{(3)})}{\det(\alpha_{mj})}, \quad B_2 = \frac{\det(\beta_{mj}^{(4)})}{\det(\alpha_{mj})}, \\
 & C_2 = \frac{\det(\beta_{mj}^{(5)})}{\det(\alpha_{mj})}, \quad D_2 = \frac{\det(\beta_{mj}^{(6)})}{\det(\alpha_{mj})}
 \end{aligned} \quad (19)$$

where the matrix  $(\beta_{mj}^{(k)})$  is obtained from the matrix  $(\alpha_{mj})$  by replacing the  $k$ -th column of the latter one with column  $(-P_0 \delta_j^1)$ .

Thus, in this way, we determine completely the Fourier transformation of the sought functions. The originals of these functions are determined from the inverse Fourier transformation

$$\begin{aligned}
 & \left\{ \sigma_{rr}^{(n)}; \sigma_{\theta\theta}^{(n)}; \sigma_{zz}^{(n)}; \sigma_{rz}^{(n)}; u_r^{(n)}; u_z^{(n)} \right\} = \\
 & \frac{1}{2\pi} \int_{-\infty}^{+\infty} \left\{ \sigma_{rrF}^{(n)}; \sigma_{\theta\theta F}^{(n)}; \sigma_{zzF}^{(n)}; \sigma_{rzF}^{(n)}; u_{rF}^{(n)}; u_{zF}^{(n)} \right\} e^{-isz} ds
 \end{aligned} \quad (20)$$

Note that the integral in (20) is calculated numerically. The algorithm for calculation of this integral we will discuss in the next section.

#### 4. Numerical results and discussions

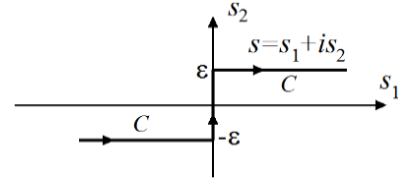


Fig. 2 The sketch of the Sommerfeld contour

In the present section, first, we consider the algorithm for calculation of the integral in (20) and consider numerical examples illustrating its validation and after these considerations we present numerical results on the frequency response of the normal and shear stresses acting on the interface surface between the constituents and discuss them.

##### 4.1 The algorithm for calculation of the integral in (20)

The integrals in (20) are called the wavenumber integrals, because if we equate to zero the  $\det(\alpha_{mj})$  in (19) and consider the Fourier transformation parameter  $s$  as the wave number, then we obtain the dispersion equation for the corresponding longitudinal axisymmetric wave propagation. In other words, the solution  $\Omega = \Omega(s)$  to the equation  $\det(\alpha_{mj}) = 0$  is the dispersion diagram of the aforementioned wave propagation. Consequently this solution is also the singular points of the integrated functions in (20), i.e., the integrated functions in (20) have singular points with respect to  $s$ , and if the order of this singularity is equal to one, then the integrals have a meaning in Cauchy's principal value sense. However, in the cases where the order of the singularity is equal to two, then these cases cause resonance type behavior of the system under consideration.

The algorithms used under calculation of the wavenumber integrals are detailed in the works by Tsang (1978), Jensen *et al.* (2011), Akbarov (2015) and others listed therein. Among these algorithms a more suitable and convenient one is the algorithm based on the use of the Sommerfeld contour. For employing this algorithm, according to Cauchy's theorem, the contour  $[-\infty, +\infty]$  is "deformed" into the contour  $C$  (Fig. 2), which is called the Sommerfeld contour in the complex plane  $s = s_1 + is_2$  and in this way the real roots of the equation  $\det(\alpha_{mj}) = 0$  are avoided. Despite this avoidance of the real roots of the equation  $\det(\alpha_{mj}) = 0$ , the values of the integrals calculated by the Sommerfeld contour algorithm have a jump in the near vicinity of the second order singular points. Such cases which appear with respect to the concrete problems as examples, are also detailed in the monograph by Akbarov (2015). Hence, this method also allows for determination of the cases in which resonance behaviors of the system take place.

Thus, according to the foregoing discussions, the integrals in (20) can be presented as follows.

$$\left\{ \sigma_{rr}^{(n)}; \sigma_{\theta\theta}^{(n)}; \sigma_{zz}^{(n)}; \sigma_{rz}^{(n)}; u_r^{(n)}; u_z^{(n)} \right\} = \quad (21)$$

$$\frac{1}{2\pi} \int_C \left\{ \sigma_{rrF}^{(n)}; \sigma_{\theta\theta F}^{(n)}; \sigma_{zzF}^{(n)}; \sigma_{rzF}^{(n)}; u_{rF}^{(n)}; u_{zF}^{(n)} \right\} e^{-isz} ds$$

Using the configuration of the contour  $C$  given in Fig. 2 we can write the following relation for the integrals in (20).

$$\begin{aligned} \int_C f(s) e^{-isz} ds &= \int_0^{+\infty} [f(s_1 + i\varepsilon) + f(-s_1 - i\varepsilon)] \\ &\quad \times \cos((s_1 + i\varepsilon)z) ds_1 - \\ &+ i \int_0^{+\infty} [f(s_1 + i\varepsilon) - f(-s_1 - i\varepsilon)] \sin((s_1 + i\varepsilon)z) ds_1 \\ &\quad + i \int_{-\varepsilon}^{+\varepsilon} f(is_2) ds_2 \end{aligned} \quad (22)$$

Assuming that  $\varepsilon \ll 1$  we can neglect the last integral on the right side of the relation (22) and use the following expression for calculation of the integrals in (20).

$$\begin{aligned} \int_C f(s) e^{-isz} ds &\approx \int_0^{+\infty} [f(s_1 + i\varepsilon) + f(-s_1 - i\varepsilon)] \\ &\quad \times \cos((s_1 + i\varepsilon)z) ds_1 - \\ &+ i \int_0^{+\infty} [f(s_1 + i\varepsilon) - f(-s_1 - i\varepsilon)] \sin((s_1 + i\varepsilon)z) ds_1. \end{aligned} \quad (23)$$

Note that under calculation of the integrals in (23) the improper integral  $\int_0^{+\infty} (\bullet) ds_1$  is replaced with the corresponding definite integral  $\int_0^{S_1^*} (\bullet) ds_1$  and the values of  $S_1^*$  are defined from the corresponding convergence requirement. At the same time, under calculation of the integral  $\int_0^{S_1^*} (\bullet) ds_1$ , the interval  $[0, S_1^*]$  is divided into a certain number (denote this number through  $N$ ) of shorter intervals and within each of these shorter intervals the integrals are calculated by the use of the Gauss algorithm with ten integration points. The values of the integrated functions at these integrated points are calculated through the solution of the Eqs. (17)-(19) and it is assumed that in each of the shorter intervals the sampling interval  $\Delta s_1$  of the numerical integration must satisfy the relation  $\Delta s_1 \ll \min\{\varepsilon, 1/z\}$ . All these procedures are performed automatically in the PC by use of the corresponding programs constructed by the authors of the paper in MATLAB. Numerical results for the problem under consideration can be also obtained with employing of the packet programs ANSYS or COMSOL. However, these programs solve the problem within the scope of the finite element modelling which is especially numerical method. Note that any analytical solution of the problem is more accurate and authentic than corresponding numerical solution and this is advantage of the used analytical-numerical method with respect to the use of the packet programs ANSYS or COMSOL. However, if we considered the problem related to the more complicated geometries for which it is difficult to find analytical or approximate analytical solutions, then, it can be appeared the necessity the use of the packet programs ANSYS or COMSOL.

## 4.2 Testing of the calculation algorithms

We test the calculation algorithm with respect to the frequency response of the normal stress

$$\sigma_{rr}(z) = \sigma_{rr}^{(1)}(R, z) = \sigma_{rr}^{(2)}(R, z) \quad (24)$$

i.e., the relation between the stress  $\sigma_{rr}$  ( $=\sigma_{rr}(0)$ ) and dimensionless frequency  $\Omega$  determined by expression (10) in the case where  $E^{(1)}/E^{(2)}=0.5$ ,  $\nu^{(1)}/\nu^{(2)}=0.3$ ,  $R/h=10$  and  $\rho^{(1)}\mu^{(1)}/\rho^{(2)}\mu^{(2)}=1$ . Consider the perfect contact case, i.e., assume that  $F=0$  in (6).

First we consider the convergence of the numerical results with respect to the number  $N$  under  $S_1^*=9$  and  $\varepsilon=0.01$ . These results are illustrated by the corresponding graphs given in Fig. 3(a). As we will also discuss below, the dependence between the stress  $\sigma_{rr}$  and  $\Omega$  has non-monotonic character and in the vicinity of  $\Omega$  at which the stress has its absolute maximum (denote this value of  $\Omega$  through  $\Omega^*$ ) the convergence of the numerical results requires a greater value of the number  $N$ . For instance, according to the results given in Fig. 3(a), the value of  $N$  (denote this value through  $N^*$ ) after which the order of the influence of an increase in the  $N$  is not greater than  $10^{-6} \div 10^{-7}$  on the stress under consideration, is  $N^*=100$  for the selected values of the problem parameters. In a similar manner, the values of  $N^*$  are determined for the other values of the problem parameters which are considered in the present paper.

Fig. 3(b) shows the convergence of the considered in Fig. 3(a) results with respect to the values of  $S_1^*$ . It follows from Fig. 3(b) that a decrease in the values of  $S_1^*$  causes a decrease of the absolute values of the stress. These values of the stress approach a certain limit one with  $S_1^*$  and as this limit the results obtained in the case where  $S_1^*=9$  can be taken, because the absolute values of the difference between the results obtained under  $S_1^*=9$  and under  $S_1^* > 9$  is not greater than  $10^{-6}$ .

Consider selection of the values of the parameter  $\varepsilon$  and note that, according to the relation  $\Delta s_1 = S_1^*/(10N) \ll \min\{\varepsilon, 1/z\}$ , as indicated above, this selection depends also on the values of  $N$  and  $S_1^*$ . Examples of the influence of  $\varepsilon$  on the frequency response of the stress  $\sigma_{rr}$  in the cases where  $E^{(1)}/E^{(2)}=1, 0.8$  and  $0.5$  are given in Fig. 3(c). The results given in Fig. 3c and others which are not given here show that to obtain sufficiently accurate results it is enough to select the value of  $\varepsilon$  from the interval  $0.0001 \leq \varepsilon \leq 0.01$ .

Taking the foregoing type of results into consideration, all the numerical results which will be discussed below are obtained in the case where  $N^*=100$ ,  $S_1^*=9$  and  $\varepsilon=0.01$ . Moreover, under obtaining these numerical results we assume that  $\nu^{(1)}/\nu^{(2)}=0.3$  and  $\rho^{(1)}\mu^{(1)}/\rho^{(2)}\mu^{(2)}=1$ .

Unfortunately we haven't found any related results in the literature with which to compare the present ones. Therefore, the foregoing numerical results can also be taken as validation of the algorithm and PC programs used in the present investigation.

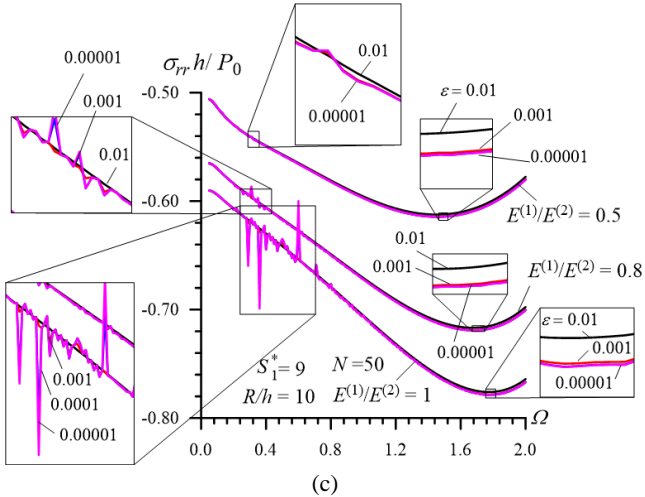
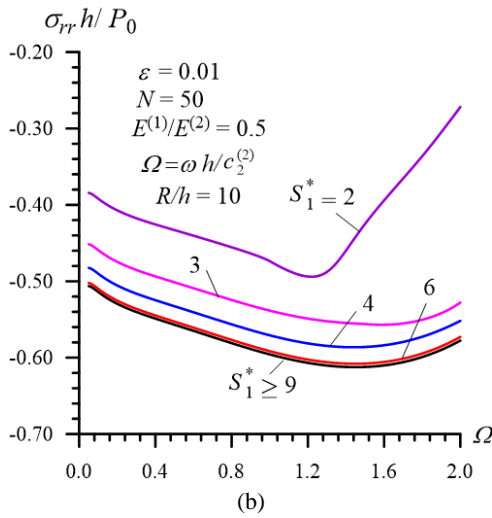
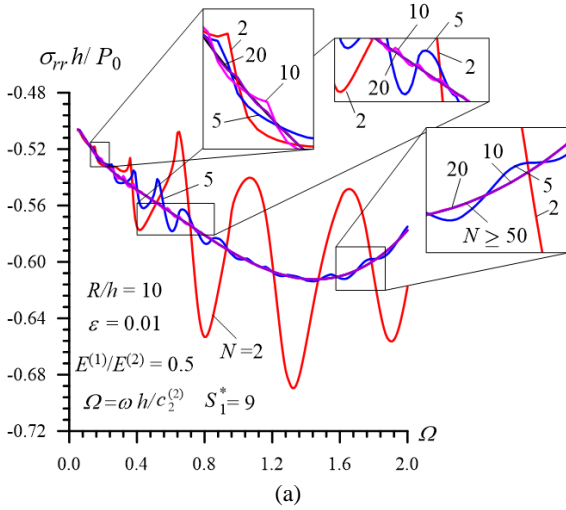


Fig. 3 Examples of the convergence of the numerical results with respect to the number  $N$  (a) to the value of  $S_1^*$  and (b) to the value of  $\varepsilon$

#### 4.3 Numerical results related to the perfect contact case

First of all, we note that the results discussed in the present subsection are obtained in the case where  $F=0$  in the

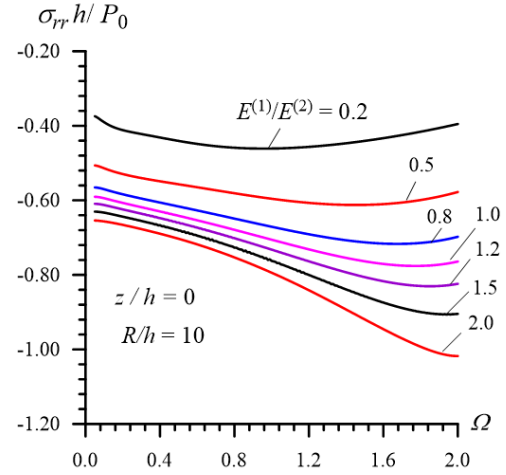


Fig. 4 Frequency response of the normal stress  $\sigma_{rr}$  obtained for various  $E^{(1)}/E^{(2)}$  under  $h/R=1/10$

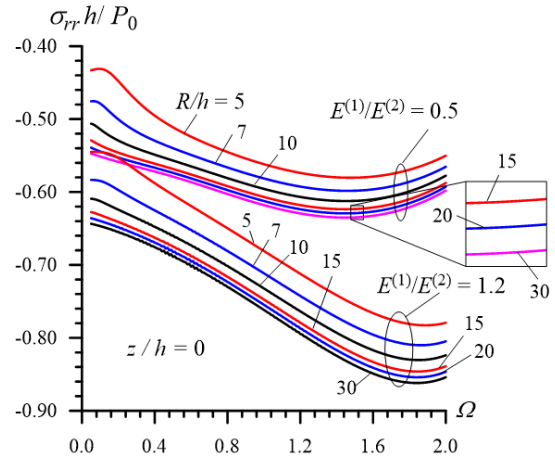


Fig. 5 Frequency response of the normal stress  $\sigma_{rr}$  obtained for various  $h/R$  under  $E^{(1)}/E^{(2)}=0.5$  and  $1.2$

condition (6). Moreover, we note that besides the normal stress  $\sigma_{rr}(z)$  determined through the expression (24), we consider also the shear stress

$$\sigma_{rz}(z) = \sigma_{rz}^{(1)}(R, z) = \sigma_{rz}^{(2)}(R, z) \quad (25)$$

which also acts on the interface surface between the constituents of the system under consideration.

Thus, we consider the frequency response of the stress  $\sigma_{rr} (= \sigma_{rr}(0))$  illustrated by the graphs given in Fig. 4 which are constructed for various values of the ratio  $E^{(1)}/E^{(2)}$  under  $h/R=1/10$ . The influence of the ratio  $h/R$  on this frequency response is illustrated by the graphs given in Fig. 5 which are constructed in the cases where  $E^{(1)}/E^{(2)}=0.5$  and  $1.2$ . The corresponding results on the frequency response of the shear stress  $\sigma_{rz} (= \sigma_{rz}(0.5))$  obtained for various  $E^{(1)}/E^{(2)}$  under  $h/R=1/10$  are given in Fig. 6. Moreover, the graphs showing the frequency response of the stress  $\sigma_{rz} (= \sigma_{rz}(0.5))$  obtained for various  $h/R$  are given in Fig. 7 which are constructed in the cases where  $E^{(1)}/E^{(2)}=0.5$  (Fig. 7(a)) and  $1.2$  (Fig. 7(b)).

Thus, it follows from Figs. 4-7 that in the considered range of change of the dimensionless frequency  $\Omega$ , i.e., in the cases where  $0 < \Omega \leq 2$ , the frequency responses of the

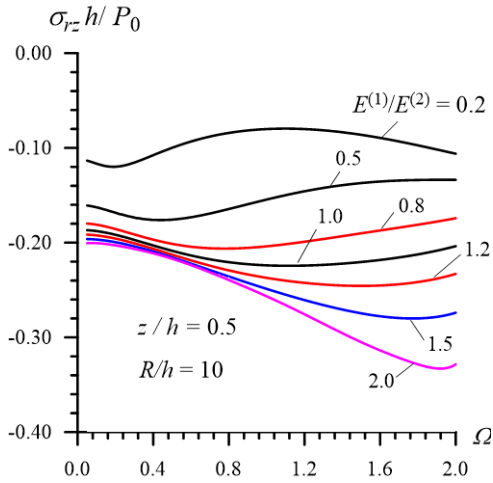


Fig. 6 Frequency response of the shear stress  $\sigma_{rz}$  obtained for various  $E^{(1)}/E^{(2)}$  under  $h/R=1/10$

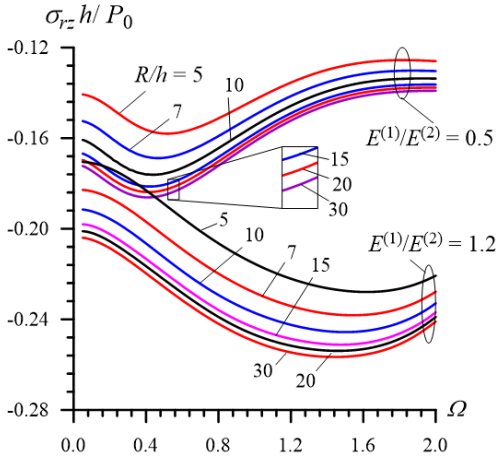


Fig. 7 Frequency response of the shear stress  $\sigma_{rz}$  obtained for various  $h/R$  under  $E^{(1)}/E^{(2)}=0.5$  and  $1.2$

stresses have non-monotone character, i.e. there exists such a value of the frequency  $\Omega$  under which absolute values of the stresses have their maximum. We call these maximums and their corresponding frequencies the “resonance” values of the stresses (denoted by  $\sigma_{rr}^*$  and  $\sigma_{rz}^*$ ) and “resonance” frequencies (denoted by  $\Omega^*$ ), respectively. Namely, according to this property of the frequency responses, it can be concluded that the behavior of the mechanical system comprising the hollow circular cylinder and surrounding elastic medium (as a time-harmonic forced vibration of the systems consisting of the covering layer and half-space (see, Akbarov 2015)) is similar to that of the system consisting of a spring, mass and parallel connected dashpot.

It follows from Figs. 4 and 6 that a decrease in the values of the ratio  $E^{(1)}/E^{(2)}$  (i.e., with increasing of the modulus of elasticity of the cylinder material under fixed modulus of elasticity of the surrounding elastic medium) causes a decrease in the absolute values of the interface stresses  $\sigma_{rr}$  and  $\sigma_{rz}$ , and their “resonance” values  $\sigma_{rr}^*$  and  $\sigma_{rz}^*$ . These figures also show that a decrease in  $E^{(1)}/E^{(2)}$  causes a decrease in the values of  $\Omega^*$ .

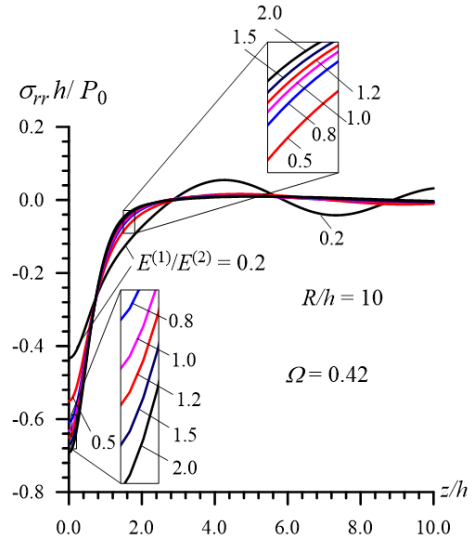


Fig. 8 Distribution of the stress  $\sigma_{rr}$  with respect to  $z/h$  in the cases where  $E^{(1)}/E^{(2)} \leq 1$  and  $E^{(1)}/E^{(2)} \geq 1$

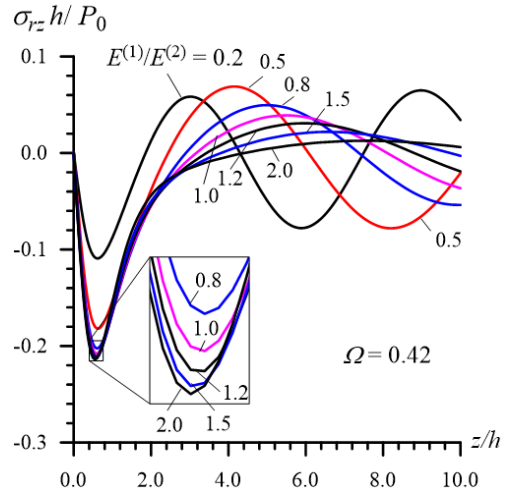


Fig. 9 Distribution of the stress  $\sigma_{rz}$  with respect to  $z/h$  in the cases where  $E^{(1)}/E^{(2)} \leq 1$  and  $E^{(1)}/E^{(2)} \geq 1$

Note that the results on the decrease of the absolute values of the interface stresses with increasing of the modulus of elasticity of cylinder layer (or covering layer) material agrees with well-known impact events of layered systems which are observed in daily engineering practice.

Moreover, note that the non-monotonic character of the dependencies between the interface stresses and dimensionless frequency  $\Omega$  is caused with the physical nature of the vibration of the system under consideration. If to say more precisely, this non-monotonic character of the mentioned dependencies is caused with infinity of the sizes of the system under consideration in the radial and axial directions. These infinities of sizes mean that there is not any reflected waves from the surfaces which bound the body. Namely, as a result of this non-reflection the ordinary resonance case does not takes place and the “resonance” cases appear instead of that.

Figs. 5 and 7 show that the absolute values of  $\sigma_{rr}$  and  $\sigma_{rr}^*$ , as well as the absolute values of  $\sigma_{rz}$  and  $\sigma_{rz}^*$  increase

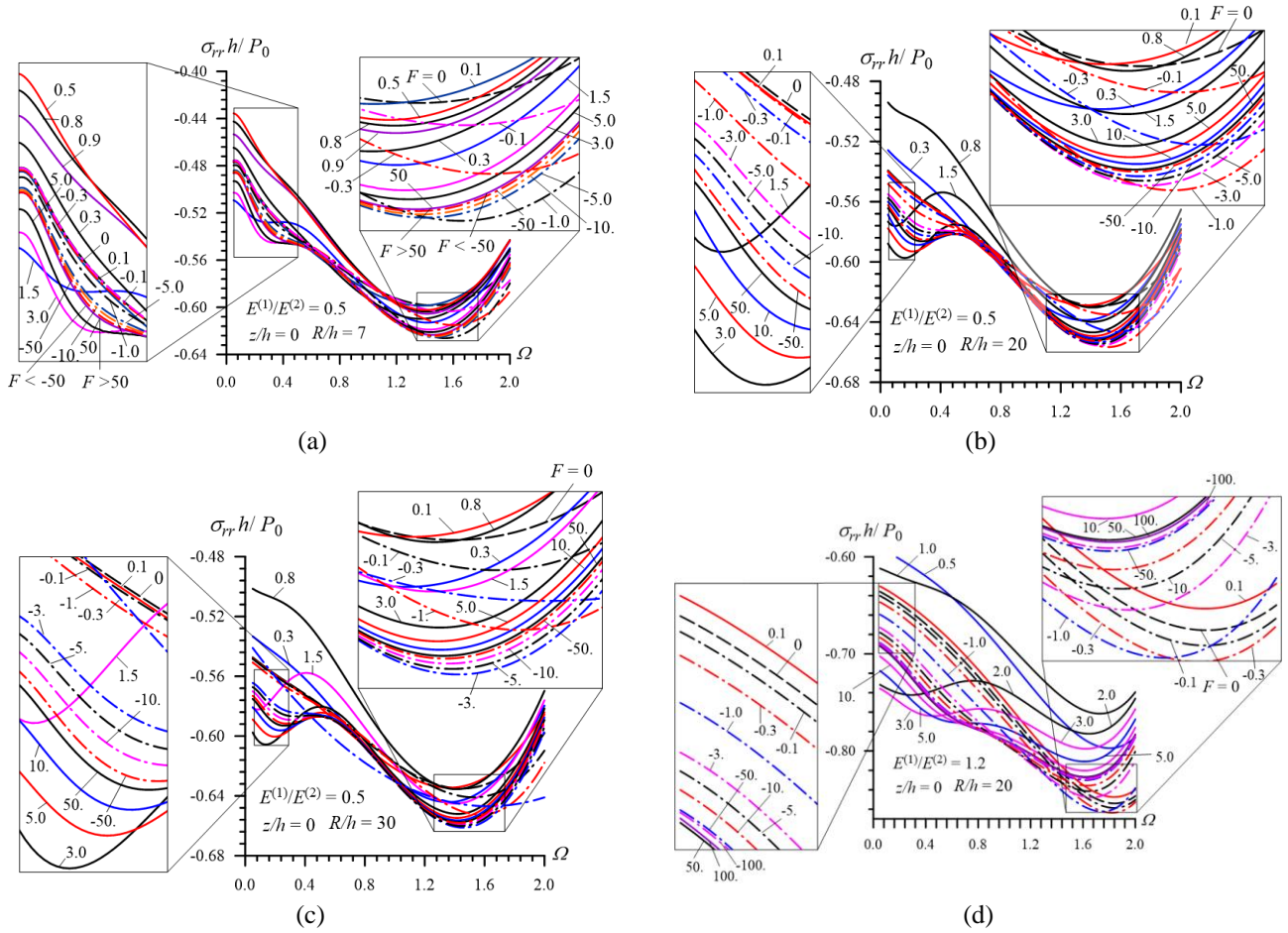


Fig. 10 The influence of the shear-spring type imperfectness of the contact conditions on the frequency response of the normal stress  $\sigma_{rr}$  the : the cases where  $h/R=1/7$  (a),  $1/20$  (b),  $1/30$  (c) under  $E^{(1)}/E^{(2)}=0.5$  and  $h/R=1/20$  under  $E^{(1)}/E^{(2)}=1.2$  (d)

with decreasing of the ratio  $h/R$  (or with increasing of the ratio  $R/h$ ), i.e., with increasing of the radius of the interface cylindrical surface under fixed thickness of the cylinder. At the same time, these figures show that in the case where  $E^{(1)}/E^{(2)}=0.5$  (in the case where  $E^{(1)}/E^{(2)}=1.2$ ) the values of the resonance frequency  $\Omega^*$  decrease (increase) with decreasing of the ratio  $h/R$ .

For avoiding the misunderstanding note that in Fig. 7 in the region  $0.01 \leq \Omega \leq 0.6$  the graph constructed for the case where  $R/h=0.5$  under  $E^{(1)}/E^{(2)}=1.2$  is crossed with the graphs constructed for the cases  $R/h=15, 20$  and  $30$  under  $E^{(1)}/E^{(2)}=0.5$  and there isn't any connection between these graphs in the sense of multi-valuation of the results.

Consider the distribution of the stresses with respect to  $z/h$ , the graphs of which are given in Figs. 8 and 9 for  $\sigma_{rr}$  and  $\sigma_{rz}$ , respectively. It follows from the results that the peak values of the stress  $\sigma_{rr}$  appear at the point  $z/h=0$ . However, the position of the point at which the peak values of the stress  $\sigma_{rz}$  appear, depends on the problem parameters, for instance on the ratio  $E^{(1)}/E^{(2)}$ . At the same time, the results show that the attenuation of the stress  $\sigma_{rz}$  with  $z/h$  depends significantly on the ratio  $E^{(1)}/E^{(2)}$ . So this attenuation becomes more significant with  $E^{(1)}/E^{(2)}$ . Moreover, it follows from Fig. 8 that the influence of the ratio  $E^{(1)}/E^{(2)}$  on the attenuation of the stress  $\sigma_{rr}$  with  $z/h$  is insignificant.

#### 4.4 Numerical results obtained in the shear-spring type imperfect contact case

The main aim of the numerical investigations considered in the present subsection, is to determine how the imperfection of the contact conditions acts in the qualitative and quantitative sense on the frequency responses of the stresses studied in the previous subsection. For this purpose we consider the numerical results on the frequency response of the stress  $\sigma_{rr}$  ( $=\sigma_{rr}(0)$ ), obtained for various values of the  $F$  in (6) under some selected values of the problem parameters. These results are given in Fig. 10 which relate to the cases where  $E^{(1)}/E^{(2)}=0.5$  (Fig. 10(a) for  $h/R=1/7$ ; Fig. 10(b) for  $h/R=1/20$  and Fig. 10(c) for  $h/R=1/30$ ) and  $E^{(1)}/E^{(2)}=1.2$  (Fig. 10(d) for  $h/R=1/20$ ).

We consider the cases  $-\infty < F \leq 0$  and  $0 < F < +\infty$  separately and which have the following meaning: according to (6), in the case where  $F > 0$  (the case where  $F < 0$ ) if  $\sigma_{rz} < 0$ ,  $u_z^{(2)} > 0$  and  $u_z^{(1)} > 0$  then the relation  $u_z^{(2)} < u_z^{(1)}$  ( $u_z^{(2)} > u_z^{(1)}$ ) occurs. It can also be presented other similar cases which have real practical meaning.

Thus, it follows from these and other results which are not given here that under  $F \rightarrow -\infty$  the results obtained in the case where  $F < 0$  approach the corresponding results obtained in the case where  $F > 0$  under  $F \rightarrow +\infty$ . This situation

can also be predicted, according to the usual mechanical consideration and according to the mathematical expression of the condition (6). Note that the results obtained for  $F=\pm\infty$  correspond the “full-slipping” contact condition, according to which, it is assumed that shear stress on the interface-contact surface is equal to zero, i.e.,  $\sigma_{rz}=0$  at  $r=R$ . Namely, according to this statement, it can be predicted that the absolute “resonance” values of the interface normal stress  $\sigma_{rr}$  obtained in the “full-slipping” contact case must be greater than corresponding ones obtained in the cases where  $|F|<\infty$ . This prediction is confirmed by the results illustrated in Fig. 10. Moreover, it follows from Fig. 10 that, in general, the character of the influence of the parameter  $F$  on the frequency response under consideration has non-monotonic and complicated character. The magnitude of this influence depends significantly on the values of the vibration frequency of the external force. For instance, the absolute values of the stresses obtained under  $\Omega\leq 1.0$  in the cases where  $F=0.5, 0.8$  and  $0.9$  for  $R/h=7$  are less than those obtained in the complete contact condition case, i.e. in the case where  $F=0$ . However, in all the considered cases the absolute “resonance” values of the normal stress obtained for the cases where  $F>0$  increase monotonically with the values of  $F$ . In this case the “resonance” frequencies (i.e. frequencies corresponding the “resonance” values of the normal stress) increase also with  $F$ . At the same time, it follows from the results given in Fig. 10 that the dependence between the absolute “resonance” values of the stress and  $|F|$  has a non-monotonic character, so that the mentioned “resonance” values increase (decrease) with  $|F|$  before (after) a certain  $F$ .

Now we present some arguments on the applications of the obtained theoretical results. It is known that the realization of the rotationally symmetric time-harmonic loading is difficult, nevertheless the theoretical results obtained within this assumption can be used as very important information on the dynamical behavior of the system under consideration. For instance, the magnitudes of the interface stresses obtained for the case under consideration can be used as an upper limit case for interface stresses obtained for each corresponding non-axisymmetric time-harmonic external loading case. Moreover, theoretical results on the influence of the material properties of the constituents of the system under consideration, as well as results on the influence of the imperfections of the contact conditions are valid also in the qualitative sense in the non-axisymmetric time-harmonic cases.

The results obtained in the present investigations have also the following application. Here we consider the steady-state axisymmetric dynamic problem and if under solution procedure of this problem we take the frequency  $\omega$  (or  $\Omega$ ) as the Fourier or Laplace transformation parameter, then the theoretical results obtained in the present paper in the cases where  $\Omega\rightarrow 0$  and  $\Omega\gg 1$  can be taken with a certain accuracy as corresponding results related to the corresponding non steady-state dynamic problem with zero initial conditions under  $t\rightarrow\infty$  and under  $t\rightarrow 0$ , respectively. As an example for such non steady-state dynamic problem it can be taken an explosion inside the pipes used in geological prospecting.

Consequently, the theoretical results obtained in the present paper have not only applications in the qualitative sense, but also these results have direct quantitative applications for the limit cases of the corresponding non stationary dynamical problem.

## 5. Conclusions

Thus, in the present paper the axisymmetric forced vibration of the system comprising the hollow cylinder and surrounding infinite elastic medium under action of the point-located time-harmonic force loaded on the inner surface of the cylinder, with respect to the cylinder’s axis and which is uniformly distributed in the circumferential direction, is investigated. This investigation is made by employing the exact equations of linear elastodynamics for isotropic bodies. It is assumed that between the constituents of the system shear-spring type imperfect contact conditions are satisfied. Numerical results on the frequency response of the normal and shear stresses acting on the interface surface between the constituents are presented and discussed. These results are obtained in two cases: in Case 1 it is assumed that the contact conditions between the constituents are perfect; in Case 2 it is assumed that shear-spring type imperfect contact conditions between the constituents take place. From the discussions of these results the following concrete conclusions can be drawn in Case 1.

- the frequency response of the stress has non-monotonic character, i.e., there exists such a value of the frequency (denoted by  $\Omega^*$  and called a “resonance” frequency) under which the absolute values of the stresses have their maximum (i.e., the “resonance” stresses appear). Consequently, the behavior of the forced vibration of the system consisting of the hollow cylinder and surrounding elastic medium is similar to that of the system consisting of a spring, mass and dashpot;
  - the “resonance” frequencies and absolute values of the normal and shear stresses decrease with increasing of the elasticity modulus of the cylinder material, however;
  - an increase of the radius of the cross section of the cylinder under constant thickness causes an increase in the absolute values of the stresses and a decrease in the values of the “resonance” frequency.
- At the same time, the numerical results obtained in Case 2 allow us to draw the following main conclusions:
- the character of the influence of the shear-spring type imperfection on the values of the interface stresses depends significantly on the vibration frequency of the external force;
  - in the cases where  $F>0$  the absolute “resonance” values of the stress increase monotonically with  $F$  and approach the corresponding ones obtained in the “full-slipping” contact case as  $F\rightarrow+\infty$ , however, in the cases where  $F<0$  the dependence between the absolute “resonance” values of the stress and  $|F|$  has a non-monotonic character and the values of the stress also approach the corresponding ones obtained in the “full-slipping” contact case as  $F\rightarrow-\infty$ .

## Acknowledgments

This study was made according to the Project No. 5/3, 2015: “Complex of theoretical and experimental investigations related to the study of the interdisciplinary problems of the Geomechanics” of the National Academy of Sciences of Azerbaijan.

## References

- Abdulkadirov, S.A. (1981), “Low-frequency resonance waves in acylindrical layer surrounded by an elastic medium”, *J. Min. Sci.*, **80**, 229-234.
- Akbarov, S.D. (2006a), “Dynamical (time-harmonic) axisymmetric interface stress field in the finite pre-strained half-space covered with the finite pre-stretched layer”, *Int. J. Eng. Sci.*, **44**, 93-112.
- Akbarov, S.D. (2006b), “On the dynamical axisymmetric stress field in a finite pre-stretched bi-layered slab resting on a rigid foundation”, *J. Sound Vib.*, **294**, 221-237.
- Akbarov, S.D. (2013), “On the axisymmetric time-harmonic Lamb’s problem for a system comprising a half-space and a covering layer with finite initial strains”, *CMES: Compos. Model. Eng. Sci.*, **70**, 93-121.
- Akbarov, S.D. (2015), *Dynamics of Pre-strained Bi-material Elastic Systems: Linearized Three-dimensional Approach*, Springer, New-York.
- Akbarov, S.D. and Guler, C. (2007), “On the stress field in a half-plane covered by the pre-stretched layer under the action of arbitrary linearly located time-harmonic forces”, *Appl. Math. Model.*, **31**, 2375-2390.
- Akbarov, S.D. and Ilhan, N. (2010), “Time-harmonic dynamical stress field in a system comprising a pre-stressed orthotropic layer and pre-stressed orthotropic half-plane”, *Arch. Appl. Mech.*, **80**, 1271-1286.
- Akbarov, S.D. and Ilhan, N. (2013), “Time-harmonic Lamb’s problem for a system comprising a piezoelectric layer and piezoelectric half-plane”, *J. Sound Vib.*, **332**, 5375-5392.
- Akbarov, S.D. and Ipek, C. (2012), “Dispersion of axisymmetric longitudinal waves in a pre-strained imperfectly bonded bi-layered hollow cylinder”, *CMC: Comput. Mater. Continua*, **32**(2), 99-144.
- Akbarov, S.D. and Ipek, C. (2015), “Influence of an imperfection of interfacial contact on the dispersion of flexural waves in a compound cylinder”, *Mech. Compos. Mater.*, **51**(2), 191-198.
- Asgari, M. and Akhlagi, M. (2011), “Natural frequency analysis of 2D-FGM thick hollow cylinder based on three-dimensional elasticity equations”, *Eur. J. Mech. A-Solid.*, **30**, 72-81.
- Baba, S. and Keles, I. (2016), “A novel approach to forced vibration behavior of thick-walled cylinders”, *Int. J. Press. Vess. Pip.*, **137**, 22-27.
- Bayon, A., Gascon, F., Medina, R., Nieves, F. J. and Salazar, F.J. (2012), “On the flexural vibration of cylinders under axial loads: Numerical and experimental study”, *J. Sound Vib.*, **331**, 2315-2333.
- Berger, J.R., Martin, P.A. and McCaffery, S.J. (2000), “Time-harmonic torsional waves in a composite cylinder with an imperfect interface”, *J. Acoust. Soc. Am.*, **107**(3), 1161-1167.
- Ebenezer, D.D., Ravichandran, K. and Padmanabdan, C. (2015), “Free and forced vibrations of hollow elastic cylinders of finite length”, *J. Acoust. Soc. Am.*, **137**(5), 2927-2938.
- Eringen, A.C. and Suhubi, E.S. (1975), *Elastodynamics, Finite motion, Vol. I: Linear Theory, Vol. II*, Academic Press, New-York.
- Gladwell, G.M.L. (1968), “The calculation of mechanical impedances related with surface of semi-infinite elastic”, *J. Sound Vib.*, **8**, 215-219.
- Hasheminejad, S.M. and Mirzaei, Y. (2011), “Exact 3D elasticity solution for free vibrations of an eccentric hollow sphere”, *J. Sound Vib.*, **330**, 229-244.
- Ilhan, N. and Koç, N. (2015), “Influence of polled direction on the stress distribution in piezoelectric materials”, *Struct. Eng. Mech.*, **54**, 955-971.
- Ipek, C. (2015), “The dispersion of the flexural waves in a compound hollow cylinder under imperfect contact between layers”, *Struct. Eng. Mech.*, **55**, 338-348.
- Jensen, F.B., Kuperman, W.A., Porter, M.B. and Schmidt, H. (2011), *Computational Ocean Acoustic*, 2<sup>nd</sup> Edition, Springer, Berlin.
- Johnson, K.L. (1985), *Contact Mechanics*, Cambridge Univ. Press, Cambridge.
- Kharouf, N. and Heyliger, P.R. (1994), “Axisymmetric free vibrations of homogeneous and laminated piezoelectric cylinders”, *J. Sound Vib.*, **174**(5), 539-561.
- Lamb, H. (1904), “On the propagation over the surface of an elastic solid”, *Philos. Trans. R Soc.*, **A203**, 1-42.
- Tsang, L. (1978), “Time-harmonic solution of the elastic head wave problem incorporating the influence of Rayleigh poles”, *J. Acoust. Soc. Am.*, **65**(5), 1302-1309.
- Wang, C.Y. and Achenbach, J.D. (1996), “Lamb’s problem for solids of general anisotropy”, *Wave Motion.*, **24**, 227-242.

CC